

Simulating initial steps of platelet aggregate formation in a cellular blood flow environment

Christian J. Spieker¹^[0000-0002-5235-9109], Konstantinos Asteriou¹, and Gábor Zaádorszky¹^[0000-0003-0150-0229]

Computational Science Lab, Informatics Institute, Faculty of Science, University of Amsterdam, Amsterdam, The Netherlands

Abstract. The mechano-chemical process of clot formation is relevant in both hemostasis and thrombosis. The initial phase of thrombus formation in arterial thrombosis can be described by the mechanical process of platelet adhesion and aggregation via hemodynamic interactions with von Willebrand factor molecules. Understanding the formation and composition of this initial blood clot is crucial to evaluate differentiating factors between hemostasis and thrombosis. In this work a cell-based platelet adhesion and aggregation model is presented to study the initial steps of aggregate formation. Its implementation upon the pre-existing cellular blood flow model HemoCell is explained in detail and the model is tested in a simple case study of initial aggregate formation under arterial flow conditions. The model is based on a simplified constraint-dependent platelet binding process that coarse-grains the most influential processes into a reduced number of probabilistic thresholds. In contrast to existing computational platelet binding models, the present method places the focus on the mechanical environment that enables the formation of the initial aggregate. Recent studies highlighted the importance of elongational flows on von Willebrand factor-mediated platelet adhesion and aggregation. The cell-resolved scale used for this model allows to account for important hemodynamic phenomena such as the formation of a red blood cell free layer and platelet margination. This work focuses on the implementation details of the model and presents its characteristic behavior at various coarse-grained threshold values.

Keywords: Platelet aggregation · Platelet adhesion · Cellular blood flow · Thrombosis · Hemostasis.

1 Introduction

Clot formation in thrombosis and hemostasis shares similar chemical pathways during the adherence and aggregation of platelets as well as the formation of fibrin reinforcements [34, 38]. While the chemical pathways are shared, under hemostasis and arterial thrombus formation, the latter has a different mechanical trigger [6, 22]. To improve treatment of pathological thrombosis, in the form of antithrombotic agents, without inhibiting bleeding cessation functionality of hemostasis, differentiating factors between the processes have to be evaluated.

Both processes, hemostasis and thrombosis, incorporate mechano-driven and chemical processes, where the former are mostly based on hemodynamic interactions between platelets and the plasma molecule von Willebrand factor (VWF), while the chemical processes involve the activation and cleavage of clotting factors enabling the catalyzation of reactions of the coagulation cascade, which ultimately leads to the reinforcement of the clot through fibrin depositions.

In hemostasis the balance between mechanical and chemical processes is mirrored in their onset sequence, from primary to secondary hemostasis, respectively [15]. In a recent work, Rhee et al. [28] showed that the onset and balance of these mechanisms significantly impact the structure of the forming thrombus, where tightly adherent platelets make up the outer most layer of a wound closing thrombus. In relation to this, work by Yakusheva et al. [46] proposed that hemostatic environments can be sites of high shear levels, which are traditionally associated with arterial thrombosis. Another recent work by Kim et al. [21] has shown that arterial thrombosis follows the same initial order of events as the healthy wound healing process in an arterial injury. In this work, a clot forming in a stenosed vessel geometry is shown to consist almost exclusively of VWF at the vessel wall, followed by an adjacent high concentration of platelets.

This initial adhesion and aggregation of platelets is mediated by VWF, revealing its A1 domain (VWF-A1) binding sites while unfolding from a globular to an extended form under shear flow. In the case of platelet adhesion to a coagulation surface, these platelet to VWF (platelet glycoprotein Ib (GPIb) α to VWF-A1) bonds can form under low shear flow with VWF adhered to adhesive glycoproteins such as collagen or fibrin. Platelet aggregation mediated by plasma suspended VWF requires a high shear environment [4, 22]. An exception to this are sites of high elongational flow which are caused by shear gradients and defined by exerting tensile forces. These elongational flow fields, which can be conceptualized as shear flow without the rotational flow proportion, are found to unfold plasma VWF at comparatively low shear rates [37, 39, 40]. Additionally, Abidin et al. recently proposed that platelets can mechanosense the rate of change in elongational flow leading to their activation [1].

The mechanical nature of initial platelet aggregate formation establishes why the hemodynamic flow conditions as well as cell interactions and distributions are crucial for its understanding. While experimental *in vivo* and *in vitro* analyses are limited in their temporal and spatial scale, computational models are increasingly employed to complement or even replace their experimental counterparts. To study the cellular effects and accurately evaluate clot composition in regards to porosity and permeability, platelet binding models are of special interest. In the past, Xu et al. presented a multi-scale cellular Potts model covering the continuum scale of thrombosis [45] and Fogelson et al. proposed to use spring and hinge forces to model platelet binding, while considering the effects of the coagulation cascade via added advection-diffusion equations [13]. Other aggregate models have used the dissipative particle method [11, 41, 42], the moving particle semi-implicit method [18, 19] and the Monte Carlo method [12]. More recently, Yazdani et al. presented a spectral element method model, which con-

siders different activation states of platelets [47]. Liu et al. used a shear-induced platelet aggregation model including immobilized and unfolded VWF as well as platelets modeled as rigid spheres [22, 23].

While existing platelet binding models cover a range of scales and blood clotting processes, they oftentimes reduce cellular complexity to save computational cost, by neglecting the presence of red blood cells or simplifying the ellipsoidal platelet shape. This in turn reduces the accuracy of the fluid mechanical predictions that are of pivotal importance to investigate mechanosensitive processes. Several cellular mechanisms contribute to the mechanical environments. The formation of a red blood cell free layer is associated with the margination of platelets, which is crucial for their deployment in aggregate formation [27, 49]. Additionally, the effects of elongational flows on binding mechanics are not considered by previous models.

In this work, a simplified platelet binding model is presented with focus on initial aggregate formation. The implementation is build on the existing cell-resolved blood flow model HemoCell [48], in the form of constraint-dependent platelet immobilization. The theoretical concept and early implementation was previously discussed by van Rooij [29]. In the following chapters the methodology is explained in detail and the model is tested in proof-of-concept case study simulations. While the case study focuses on initial aggregate growth in arterial thrombosis, the structure of the model allows for the simulation of different scenarios, including hemostatic platelet adhesion and aggregation, via adjustment of the individual constraint parameters. This work focuses on the implementation details and methodology of the model and its characteristic behavior is presented at various coarse-grained threshold values.

2 Initial platelet aggregate formation model

The cell-based platelet adhesion and aggregation model presented in this work is built upon the cell-resolved blood flow model HemoCell. Its fundamental concept is based on previous work by van Rooij [29], and its implementation are described in the following paragraphs. While the constraint-dependent nature of the model allows for the adjustment of threshold parameters to simulate different environments for aggregate formation, the presented work focuses on initial clot formation in arterial thrombosis.

2.1 Conceptual model considerations

HemoCell The aggregate formation model is added upon the open-source framework HemoCell. The cellular blood flow model couples a discrete element method membrane solver to the lattice Boltzmann method-based fluid solver via the immersed boundary method. In the current state the model includes membrane models for platelets and red blood cells, which can be initialized at different concentrations in a predefined geometry. The single cell and bulk flow behavior of the model were previously validated by Závodszy et al. [48]. Furthermore,

HemoCell has found a wide field of application such as modelling the flow of diabetic and healthy human as well as mouse blood in a variety of geometries and differing in their complexity [8–10, 30, 31, 39, 49].

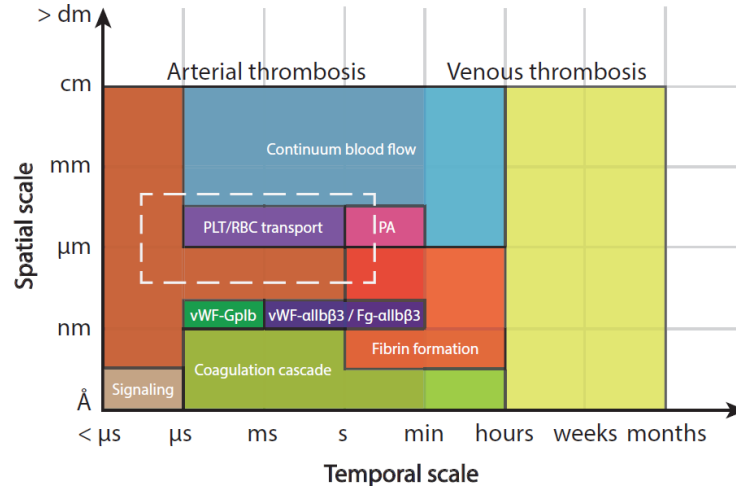


Fig. 1. HemoCell scale separation map. The dashed line represents the range of operation for HemoCell. Therefore, the processes occurring below this scale are represented in a coarse-grained fashion. 'PA' denotes platelet aggregation. Adapted with permission from van Rooij [29].

The temporal and spatial scale covered by HemoCell are visualized in the scale separation map in Figure 1. The temporal resolution up to the order of seconds and spatial resolution up to $500\ \mu\text{m}$ are in the necessary ranges to cover initial platelet aggregate formation in arterial thrombosis.

Model concept In line with the scale of operation of HemoCell, the presented model focuses on the initial phase of platelet aggregate formation, excluding the subsequent mechanisms of platelet activation, the coagulation cascade and fibrin formation. Furthermore, the adherence of red blood cells can be omitted since in arterial thrombosis, which typically leads to a platelet-rich thrombus, red blood cells assume a passive function in aggregate formation [5]. The initial phase of this aggregate formation can be described as a mechanically driven process, regulated by hemodynamic thresholds in the flow environment. The process consists of platelets binding to a thrombogenic surface, known as platelet adhesion and to each other, in the form of platelet aggregation. Initial platelet adhesion and aggregation in the high shear environment of arterial thrombosis is mediated by bonds between VWF-A1 to the platelet receptor GPIb α of the GPIb-IX-V complex [32, 35, 43].

In the proposed model, initial aggregate formation relies on the constraint-dependent immobilization of platelets, coarse-graining the process of VWF-mediated platelet adhesion and aggregation into a probabilistic threshold dependent on the local fluid mechanics. The model includes three threshold constraints - shear rate, rate of elongation and distance - which will induce the immobilization of individual platelets when reached. The numerical implementation of platelet immobilization is a process denoted as 'solidification' during which the location of the immobilized platelet is turned into a solid boundary. Additional to three constraints, a solidification probability is added as a further calibration and scaling parameter.

2.2 Model design and implementation

Binding sites Platelet adhesion to a thrombogenic surface, such as collagen, fibronectin or laminin is a necessity for subsequent platelet aggregation [32]. In the model, the thrombogenic surface is defined as a list of boundary nodes of the simulated domain wall, labeled as *BindingSites*. For the immobilization of platelets in the solidification process, the vicinity of each binding site node is searched for platelets that reach the threshold constraints. The platelets that are solidified become binding sites for other platelets and their nodes are therefore added to the *BindingSites* list (see Figure 2 (b) and (c)).

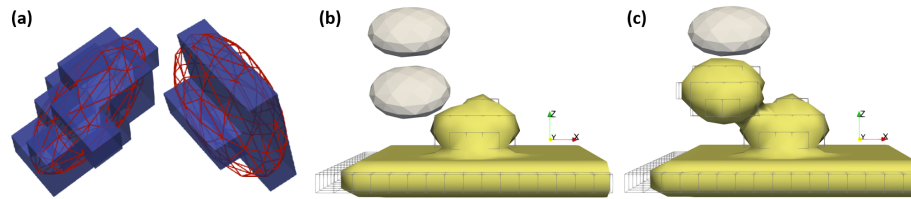


Fig. 2. Platelet solidification process. (a): Two platelets (in red) with the inner fluid nodes determined using the even-odd rule (in blue). Adapted with permission from van Rooij [29]. (b) & (c): Solidification process, with one and two solidified platelets, respectively. The boundary contours of the binding site (in yellow) are surrounded by a wireframe view of boundary nodes.

Constraints The included constraints are shear rate, rate of elongation and distance to the closest binding site, which are evaluated for platelets in vicinity to binding sites. The distance at which a platelet solidifies includes the platelet-VWF bond length, since the mediating VWF is not explicitly modeled. While the bond length between VWF and GPIIb α is around 100 nm, VWF molecules unfolded under shear flow are shown to extend to a contour length of up to 250 μm [25, 40]. In this model a distance threshold of 1.5 μm is chosen, which is

sufficiently resolved by the immersed boundary method that couples the particles with the fluid in HemoCell, since it is three times the length of one lattice node. Each platelet that has a $\leq 1.5 \mu\text{m}$ large distance from at least one of its membrane nodes to the closest binding site is evaluated for the local shear rate and rate of elongation.

For the shear rate, a threshold of 1000 s^{-1} is defined, which is in line with values where immobilized VWF begins to unfold [14, 33]. Although, shear-induced platelet aggregation, mediated via plasma suspended VWF, occurs at much higher shear rates around 5000 s^{-1} , the lower value is chosen, since platelet adhesion to a thrombogenic surface is the initial step of aggregate formation and the model does not differentiate between binding sites of the initial thrombogenic surface and binding sites of solidified platelets [36]. Additionally, the rate of elongation threshold is set to 300 s^{-1} , which corresponds to the critical value for VWF unfolding, determined by Sing et al.[37]. The shear rate threshold is evaluated based on the strain rate of the fluid nodes overlapping with the respective platelets. The largest difference in principal strain rates, calculated as the eigenvalues of the strain rate tensor, is used as the shear rate of the specific node and is compared to the defined threshold. The rate of elongation is calculated as the magnitude of the diagonal elements of the rate of strain tensor of the inner platelet nodes. If the platelet in close distance to a binding site experiences shear rates $\geq 1000 \text{ s}^{-1}$ or elongational flows $\geq 300 \text{ s}^{-1}$ it becomes a candidate for solidification. The constraint parameters are summarized in Table 1.

Table 1. Solidification constraints. The comparison operator preceding the threshold value refers to the comparison from actual to threshold value. In order to mark a platelet for solidification the distance threshold comparison and at least one of the flow threshold comparisons, shear rate or rate of elongation, have to be true.

Constraint	Threshold value	Reference(s)
Distance	$\leq 1.5 \mu\text{m}$	[25, 40]
Shear rate	$\geq 1000 \text{ s}^{-1}$	[14, 33]
Rate of elongation	$\geq 300 \text{ s}^{-1}$	[37, 39]

Solidification probability The candidate platelets that reach the threshold constraints are tagged for solidification with a predefined probability, labeled *solidificationProbability*, between 0 and 1. This parameter serves as a calibration and scaling parameter and represents the binding affinity of the modeled platelet adhesion and aggregation process [2]. To implement this binding affinity in HemoCell, platelets that reach the thresholds of the set constraints (see Table 1) are only tagged for solidification if a generated (pseudo-)random number is below the defined *solidificationProbability* value of the range of generated numbers (between 0 and *rand_max*). Otherwise, the respective platelet is not considered for solidification in the current iteration. The plot in Figure 3 visualizes the effect of the *solidificationProbability* value on the time of solidification.

For a probability of 1 the solidification delay Δt is 0 s, since a platelet eligible for solidification will be tagged and subsequently solidified immediately. With decreasing probability, the mean delay and its standard deviation increase steeply. The resolution of the solidification delay is limited by the time step of 1^{-7} s defined in HemoCell. For initial assessment of the model, the *solidificationProbability* parameter is set to 0.5.

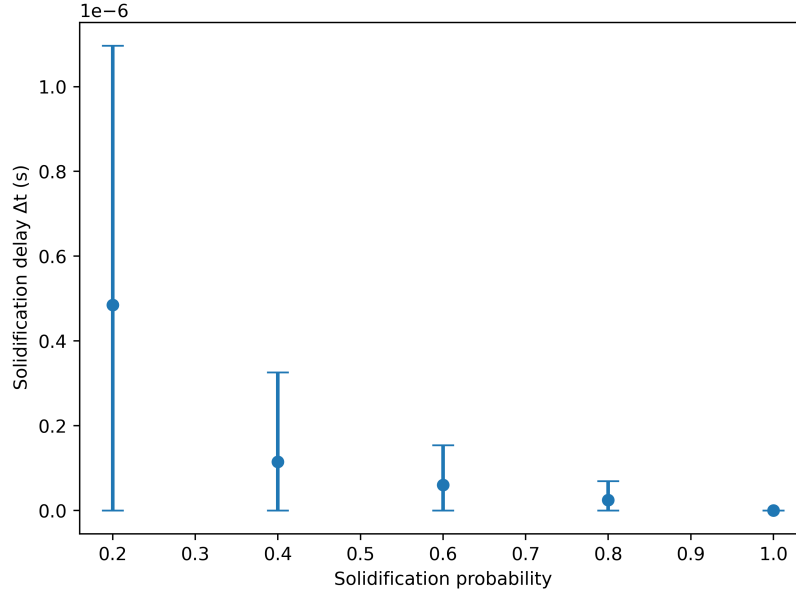


Fig. 3. Solidification probability vs. solidification delay Δt . The plot is based on single platelet simulations. To isolate the effects of the *solidificationProbability*, the platelet reaches the thresholds of the set constraints (see Table 1) at every iteration. Each measured value is based on 20 simulations.

Solidification Platelet solidification is the numerical implementation of platelet immobilization as a consequence of binding during adhesion and aggregation. The platelets tagged for solidification are converted to solid wall boundary nodes and added to the *bindingSites* list in the subsequent iteration. This 'conversion' is performed by establishing which fluid nodes the platelet intersects with and changing them to solid boundary nodes. These nodes at the position of the platelet to be solidified (see Figure 2 (a)) are determined via ray casting by applying the even-odd rule. This method was previously used by De Haan et al. to identify the internal fluid nodes of a red blood cell in order to change their viscosity to match the increased viscosity of hemoglobin [16]. The intersections between a ray and a polygon, in this case a triangle on the surface of a platelet, is determined by the Möller-Trumbore ray-triangle intersection algorithm [26]. The

ray is cast from an arbitrary distant point outside the respective shape, in this case the cell, towards the point to be tested for being within the shape or outside. To improve performance of this operation, the ray casting is fixed in its direction and an octree data structure is used to create a spatial subdivision of the triangle vertices [24]. The sum of intersections are counted for each node. An even sum places the point outside the platelet and if the number is odd; it is located inside the platelet. The identified internal nodes are converted to boundary nodes and added to the *bindingSites* list, as displayed in Figure 2 (b) and (c). From the subsequent iteration they are considered as binding sites themselves and their surface is made available for further platelets to bind to.

3 Case study

Simulation setup To assess the functionality and evaluation process of the presented model, a 'case study' simulation is set up. The simulated domain, shown in Figure 4, is based on the parallel plate flow chamber design commonly used in microfluidics to study shear-dependent platelet adhesion and aggregation [17, 20]. The setup consists of a 100 μm long channel with a width and height of 50 and 62.5 μm , respectively. In order to mimic the center of a parallel plate flow chamber, the domain utilizes periodic boundary conditions along the width (y-axis). The central 90 μm of the top channel wall are initialized as binding sites (see yellow section of channel wall in Figure 4). Additionally, a 25 x 50 x 62.5 μm^3 large periodic pre-inlet supplies the inlet of the domain with a constant inflow of cells, preventing a decrease in platelet concentration due to solidification of platelets in aggregate formation [3, 39]. Furthermore, with regular periodic boundary conditions in the flow direction, a growing aggregate could affect the surrounding cellular flow conditions and therefore possibly distort the aggregate formation results.

The pre-inlet is initialized with 162 red blood cells and 157 platelets, corresponding to a discharge hematocrit of 25%. In order to study the effects of shear rate magnitude on the initial aggregate formation, two cases with differing flow velocities are defined. The simulated flow is set up to yield a Reynolds number of 0.75 and 0.6, leading to initial wall shear rates of around 1350 and 1000 s^{-1} , respectively. The final simulations are executed on 2 nodes (consisting of 128 cores each) on the Snellius supercomputer (SURF, Amsterdam, Netherlands; <https://www.surf.nl/en/dutch-national-supercomputer-snellius>) with an average performance of 0.049 ± 0.001 s/iteration. Before simulating cellular flow and platelet binding in the entire domain, flow is simulated in the pre-inlet exclusively, to converge from the random initial cell packing towards a marginated state. The shortened domain for this 'warm-up' simulation excludes the binding sites and has the added benefit of reduced computational cost.

Simulation results Figure 5 displays the boundary contours of the solidified platelets for the two simulated cases. The difference in flow conditions causes different initial aggregate formations. The $\text{Re} = 0.75$ simulation creates a 35%

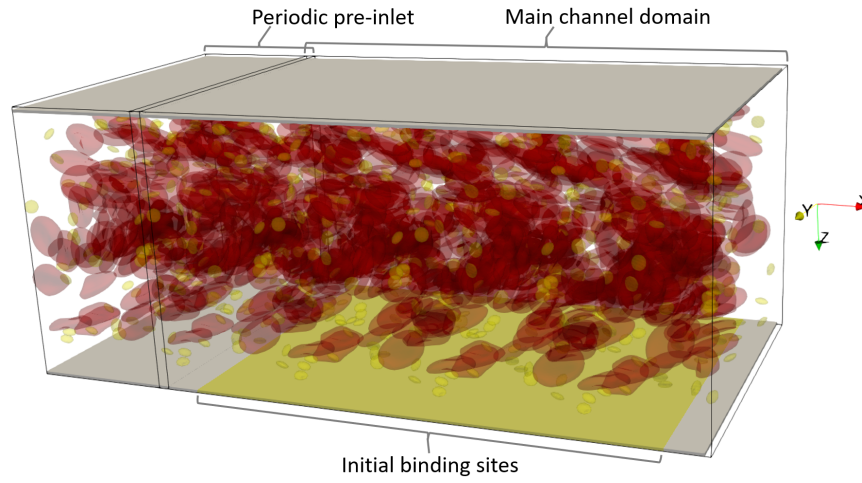


Fig. 4. Case study setup. Simulation domain with periodic pre-inlet and binding site location (in yellow). Defined flow direction is the positive x-direction. The red blood cells and platelets displayed in the channel domain are visualized at 30% opacity.

longer (in x-direction) and 35% higher (in z-direction) aggregate, than the $Re = 0.6$ simulation. While the aggregate in the $Re = 0.75$ simulation formed close to the domain inlet, the $Re = 0.6$ simulation aggregate formed at the center of the channel. As the color scale in Figure 5 showcases, this difference also affects the shear rate applied to the surface of the aggregates. The $Re = 0.75$ simulation aggregate experiences higher shear rates on a larger area, due to protruding deeper into the channel. Both cases exhibit aggregate formations that extend towards the oncoming flow direction. Furthermore, both aggregates are connected to only a single platelet that solidified upon close enough contact to the initial binding site area and all additional solidifications of the aggregates occurred within binding distance to previously solidified platelets. In addition to the aggregates shown in Figure 5, the $Re = 0.6$ simulation exhibits one additional solidified platelet close to the channel outlet.

4 Discussion

The presented work explains the methodology of a cellular platelet adhesion and aggregation model. The model is build upon the pre-existing cell-resolved blood flow framework HemoCell and focuses on simulating the mechanical process of initial platelet aggregate formation, realized via constraint-dependent platelet immobilization. The model considers red blood cells and their effect on platelet distribution, as well as the role of elongational flows in VWF-mediated platelet adhesion and aggregation, distinguishing it from previous models.

The case study simulations act as a proof-of-concept of the model and its implemented functionalities. Furthermore, the simulations show that flow condi-

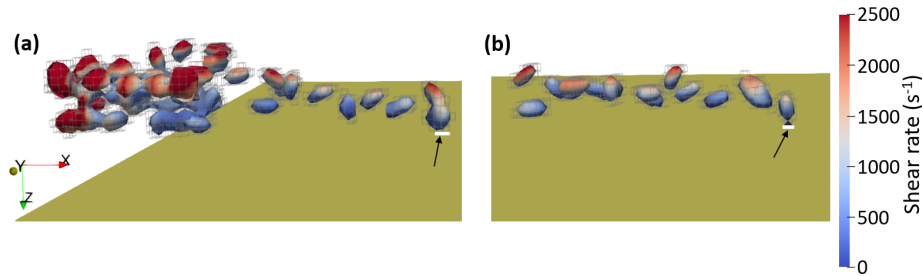


Fig. 5. Case study evaluation. (a) & (b): Boundary contour of solidified platelets, for the $Re = 0.75$ and $Re = 0.6$ simulations, respectively. The color scale represents the shear rate applied to the surface of the aggregates. Both results are captured after 0.15 s of simulated flow. The arrows point towards the area of connection (in white) of the first solidified platelet to the initial binding site area (in yellow).

tions impact the aggregate shape in the model. The implementation in HemoCell allows for extensive evaluation of cellular distributions, flow conditions and aggregate properties, such as forces acting on the solidified platelets, aggregate volume, aggregate growth over time, porosity and permeability, among others. Additionally, the model allows for adjustments of the clotting environment in regards to channel geometry, flow conditions and platelet immobilization constraints. These clotting environments can cover sites of arterial thrombosis, like a stenosed vessel section, as well as hemostatic environments, such as an injured vessel.

The larger aggregate size observed in the higher flow velocity case study simulation (see Figure 5 (a)) could be explained by an increased likelihood of platelets reaching the shear threshold as well as more platelets passing by the binding sites, as both arguments are dependent on flow velocity. Though in order to verify these results and apply the model to investigate initial platelet aggregate formation in different clotting environments, its validation is required. Complete validation is a currently ongoing effort that is performed by comparing simulated results of the model to experimental aggregate formations. Additionally, decoupling the initial binding sites, acting as the thrombogenic surface, from binding sites in the form of solidified platelets, could increase accuracy of the model. Platelet solidifications occurring in the vicinity of the initial binding sites represent platelet adhesion, whereas platelets solidifying close to previously solidified platelets depict platelet aggregation. While both processes can be mediated by VWF, they require different flow environments [32]. By decoupling their coarse-grained representation in the model, the mechanical thresholds for VWF elongation, namely distance, shear rate and rate of elongation, could be defined separately. The current simplified implementation could explain why the aggregates of both case study simulations are structured upon a single platelet - thrombogenic surface bond and their subsequent shape extends into the on-

coming flow direction. An additional simplification of the model is the solid and constant modeling of a platelet bond. In reality, platelet aggregates are slightly deformable and active structures that exhibit contraction over time. Furthermore, depending on the strength of the bond, platelets can detach from an aggregate, individually or in bulk [44]. Explicitly modeling the platelet bonds, for example with a bead-spring model, could further increase accuracy of the model.

The original model concept idea by van Rooij included the usage of so called CEPAC (Combined Effect of Pro- and Anticoagulants) fields [29]. Implemented as advection-diffusion fields to reduce the amount of free parameters in the model, the CEPAC fields are set to model the secretion of agonists by activated platelets (CEPAC1), as well as pro- and anticoagulants of the coagulation cascade (CEPAC2). Combined with different activation states of platelets, these additions to the model could widen its focus from an initial aggregate model to a more complete thrombosis and hemostasis model. To cover the large temporal scale from initial platelet adhesion to coagulation and fibrin formation (see Figure 1), increasing the reaction rates and the total platelet count could accelerate aggregate growth. Ultimately, scale bridging techniques, such as time splitting or amplification could be applied in a multiscale model approach [7].

5 Conclusion

The introduced cellular platelet adhesion and aggregation model offers a platform to investigate initial platelet aggregate formation in individually defined aggregation environments. Its constraint-dependent structure is an adjustable and modular addition to the cellular blood flow framework HemoCell. While the presented case study simulations showcase the functionality of the model and already hint towards the importance of hemodynamic flow conditions in initial aggregate formation, further calibration and validation of the model is required before significant conclusions can be made.

Acknowledgements C.J.S., K.A. and G.Z. acknowledge financial support by the European Union Horizon 2020 research and innovation programme under Grant Agreement No. 675451, the CompBioMed2 Project. C.J.S., K.A. and G.Z. are funded by CompBioMed2. The use of supercomputer facilities in this work was sponsored by NWO Exacte Wetenschappen (Physical Sciences).

References

1. Abidin, N.A.Z., Timofeeva, M., Szydzik, C., Akbaridoust, F., Lav, C., Marusic, I., Mitchell, A., Hamilton, J.R., Ooi, A.S., Nesbitt, W.S.: A microfluidic method to investigate platelet mechanotransduction under extensional strain. *Research and Practice in Thrombosis and Haemostasis* p. 100037 (jan 2023). <https://doi.org/10.1016/j.rpth.2023.100037>

2. Auton, M., Zhu, C., Cruz, M.A.: The mechanism of VWF-mediated platelet GPIIb α binding. *Biophysical Journal* **99**(4), 1192–1201 (aug 2010). <https://doi.org/10.1016/j.bpj.2010.06.002>
3. Azizi Tarksalooeyeh, V.W., Závodszy, G., van Rooij, B.J., Hoekstra, A.G.: Inflow and outflow boundary conditions for 2d suspension simulations with the immersed boundary lattice boltzmann method. *Computers & fluids* **172**, 312–317 (2018)
4. Bergmeier, W., Hynes, R.O.: Extracellular matrix proteins in hemostasis and thrombosis. *Cold Spring Harbor Perspectives in Biology* **4**(2), a005132–a005132 (sep 2011). <https://doi.org/10.1101/cshperspect.a005132>
5. Byrnes, J.R., Wolberg, A.S.: Red blood cells in thrombosis. *Blood* **130**(16), 1795–1799 (oct 2017). <https://doi.org/10.1182/blood-2017-03-745349>
6. Casa, L.D., Ku, D.N.: Thrombus formation at high shear rates. *Annual Review of Biomedical Engineering* **19**(1), 415–433 (jun 2017). <https://doi.org/10.1146/annurev-bioeng-071516-044539>
7. Chopard, B., Falcone, J.L., Kunzli, P., Veen, L., Hoekstra, A.: Multiscale modeling: recent progress and open questions. *Multiscale and Multidisciplinary Modeling, Experiments and Design* **1**(1), 57–68 (jan 2018). <https://doi.org/10.1007/s41939-017-0006-4>
8. Czaja, B., Závodszy, G., Tarksalooeyeh, V.A., Hoekstra, A.G.: Cell-resolved blood flow simulations of saccular aneurysms: effects of pulsatility and aspect ratio. *Journal of The Royal Society Interface* **15**(146), 20180485 (sep 2018). <https://doi.org/10.1098/rsif.2018.0485>
9. Czaja, B., de Bouter, J., Heisler, M., Závodszy, G., Karst, S., Sarunic, M., Maberley, D., Hoekstra, A.: The effect of stiffened diabetic red blood cells on wall shear stress in a reconstructed 3d microaneurysm. *Computer Methods in Biomechanics and Biomedical Engineering* pp. 1–19 (feb 2022). <https://doi.org/10.1080/10255842.2022.2034794>
10. Czaja, B., Gutierrez, M., Závodszy, G., de Kanter, D., Hoekstra, A., Eniola-Adefeso, O.: The influence of red blood cell deformability on hematocrit profiles and platelet margination. *PLOS Computational Biology* **16**(3), e1007716 (mar 2020). <https://doi.org/10.1371/journal.pcbi.1007716>, <https://dx.plos.org/10.1371/journal.pcbi.1007716>
11. Filipovic, N., Kojic, M., Tsuda, A.: Modelling thrombosis using dissipative particle dynamics method. *Philosophical Transactions of the Royal Society A: Mathematical, Physical and Engineering Sciences* **366**(1879), 3265–3279 (jul 2008). <https://doi.org/10.1098/rsta.2008.0097>
12. Flamm, M.H., Sinno, T., Diamond, S.L.: Simulation of aggregating particles in complex flows by the lattice kinetic monte carlo method. *The Journal of Chemical Physics* **134**(3), 034905 (jan 2011). <https://doi.org/10.1063/1.3521395>
13. Fogelson, A.L., Guy, R.D.: Immersed-boundary-type models of intravascular platelet aggregation. *Computer Methods in Applied Mechanics and Engineering* **197**(25-28), 2087–2104 (apr 2008). <https://doi.org/10.1016/j.cma.2007.06.030>
14. Fu, H., Jiang, Y., Yang, D., Scheiflinger, F., Wong, W.P., Springer, T.A.: Flow-induced elongation of von willebrand factor precedes tension-dependent activation. *Nature Communications* **8**(1) (aug 2017). <https://doi.org/10.1038/s41467-017-00230-2>
15. Gale, A.J.: Continuing education course #2: Current understanding of hemostasis. *Toxicologic Pathology* **39**(1), 273–280 (nov 2010). <https://doi.org/10.1177/0192623310389474>

16. de Haan, M., Zavodszky, G., Azizi, V., Hoekstra, A.: Numerical investigation of the effects of red blood cell cytoplasmic viscosity contrasts on single cell and bulk transport behaviour. *Applied Sciences* **8**(9), 1616 (sep 2018). <https://doi.org/10.3390/app8091616>
17. Hao, Y., Závodszky, G., Tersteeg, C., Barzegari, M., Hoekstra, A.G.: Image-based flow simulation of platelet aggregates under different shear rates (feb 2023). <https://doi.org/10.1101/2023.02.22.529480>
18. Kamada, H., Imai, Y., Nakamura, M., Ishikawa, T., Yamaguchi, T.: Computational study on thrombus formation regulated by platelet glycoprotein and blood flow shear. *Microvascular Research* **89**, 95–106 (sep 2013). <https://doi.org/10.1016/j.mvr.2013.05.006>
19. Kamada, H., ichi Tsubota, K., Nakamura, M., Wada, S., Ishikawa, T., Yamaguchi, T.: A three-dimensional particle simulation of the formation and collapse of a primary thrombus. *International Journal for Numerical Methods in Biomedical Engineering* **26**(3-4), 488–500 (mar 2010). <https://doi.org/10.1002/cnm.1367>
20. Kent, N.J., Basabe-Desmonts, L., Meade, G., MacCraith, B.D., Corcoran, B.G., Kenny, D., Ricco, A.J.: Microfluidic device to study arterial shear-mediated platelet-surface interactions in whole blood: reduced sample volumes and well-characterised protein surfaces. *Biomedical Microdevices* **12**(6), 987–1000 (jul 2010). <https://doi.org/10.1007/s10544-010-9453-y>
21. Kim, D.A., Ku, D.N.: Structure of shear-induced platelet aggregated clot formed in an in vitro arterial thrombosis model. *Blood Advances* **6**(9), 2872–2883 (may 2022). <https://doi.org/10.1182/bloodadvances.2021006248>
22. Liu, Z.L., Ku, D.N., Aidun, C.K.: Mechanobiology of shear-induced platelet aggregation leading to occlusive arterial thrombosis: A multi-scale in silico analysis. *Journal of Biomechanics* **120**, 110349 (may 2021). <https://doi.org/10.1016/j.jbiomech.2021.110349>
23. Liu, Z.L., Bresette, C., Aidun, C.K., Ku, D.N.: SIPA in 10 milliseconds: VWF tentacles agglomerate and capture platelets under high shear. *Blood Advances* **6**(8), 2453–2465 (apr 2022). <https://doi.org/10.1182/bloodadvances.2021005692>
24. Meagher, D.: Geometric modeling using octree encoding. *Computer Graphics and Image Processing* **19**(2), 129–147 (jun 1982). [https://doi.org/10.1016/0146-664x\(82\)90104-6](https://doi.org/10.1016/0146-664x(82)90104-6)
25. Mody, N.A., King, M.R.: Platelet adhesive dynamics. part II: High shear-induced transient aggregation via GPIIb α -vWF-GPIIb α bridging. *Biophysical Journal* **95**(5), 2556–2574 (sep 2008). <https://doi.org/10.1529/biophysj.107.128520>
26. Möller, T., Trumbore, B.: Fast, minimum storage ray/triangle intersection. In: *ACM SIGGRAPH 2005 Courses on - SIGGRAPH '05*. ACM Press (2005). <https://doi.org/10.1145/1198555.1198746>
27. Qi, Q.M., Shafiq, E.S.G.: Theory to predict particle migration and margination in the pressure-driven channel flow of blood. *Physical Review Fluids* **2**(9), 093102 (sep 2017). <https://doi.org/10.1103/physrevfluids.2.093102>
28. Rhee, S.W., Pokrovskaya, I.D., Ball, K.K., Ling, K., Vedanaparti, Y., Cohen, J., Cruz, D.R.D., Zhao, O.S., Aronova, M.A., Zhang, G., Kamykowski, J.A., Leapman, R.D., Storrie, B.: Venous puncture wound hemostasis results in a vaulted thrombus structured by locally nucleated platelet aggregates. *Communications Biology* **4**(1) (sep 2021). <https://doi.org/10.1038/s42003-021-02615-y>
29. van Rooij, B.J.M.: Platelet adhesion and aggregation in high shear blood flow: An insilico and in vitro study. Ph.D. thesis, Universiteit van Amsterdam (2020)

30. van Rooij, B.J.M., Závodszy, G., Azizi Tarksalooyeh, V.W., Hoekstra, A.G.: Identifying the start of a platelet aggregate by the shear rate and the cell-depleted layer. *Journal of The Royal Society Interface* **16**(159), 20190148 (oct 2019). <https://doi.org/10.1098/rsif.2019.0148>, <https://royalsocietypublishing.org/doi/10.1098/rsif.2019.0148>
31. van Rooij, B.J.M., Závodszy, G., Hoekstra, A.G., Ku, D.N.: Haemodynamic flow conditions at the initiation of high-shear platelet aggregation: a combined in vitro and cellular in silico study. *Interface Focus* **11**(1), 20190126 (2 2021). <https://doi.org/10.1098/rsfs.2019.0126>, <https://royalsocietypublishing.org/doi/10.1098/rsfs.2019.0126>
32. Ruggeri, Z.M., Mendolicchio, G.L.: Adhesion mechanisms in platelet function. *Circulation Research* **100**(12), 1673–1685 (jun 2007). <https://doi.org/10.1161/01.res.0000267878.97021.ab>
33. Ruggeri, Z.M., Orje, J.N., Habermann, R., Federici, A.B., Reininger, A.J.: Activation-independent platelet adhesion and aggregation under elevated shear stress. *Blood* **108**(6), 1903–1910 (9 2006). <https://doi.org/10.1182/blood-2006-04-011551>, <https://ashpublications.org/blood/article/108/6/1903/22637/Activation-independent-platelet-adhesion-and>
34. Sang, Y., Roest, M., de Laat, B., de Groot, P.G., Huskens, D.: Interplay between platelets and coagulation. *Blood Reviews* **46**, 100733 (mar 2021). <https://doi.org/10.1016/j.blre.2020.100733>
35. Savage, B., Saldívar, E., Ruggeri, Z.M.: Initiation of platelet adhesion by arrest onto fibrinogen or translocation on von willebrand factor. *Cell* **84**(2), 289–297 (jan 1996). [https://doi.org/10.1016/s0092-8674\(00\)80983-6](https://doi.org/10.1016/s0092-8674(00)80983-6)
36. Schneider, S.W., Nuschele, S., Wixforth, A., Gorzelanny, C., Alexander-Katz, A., Netz, R.R., Schneider, M.F.: Shear-induced unfolding triggers adhesion of von willebrand factor fibers. *Proceedings of the National Academy of Sciences* **104**(19), 7899–7903 (may 2007). <https://doi.org/10.1073/pnas.0608422104>
37. Sing, C.E., Alexander-Katz, A.: Elongational Flow Induces the Unfolding of von Willebrand Factor at Physiological Flow Rates. *Biophysical Journal* **98**(9), L35–L37 (5 2010). <https://doi.org/10.1016/j.bpj.2010.01.032>, <https://linkinghub.elsevier.com/retrieve/pii/S0006349510001979>
38. Smith, S.A., Travers, R.J., Morrissey, J.H.: How it all starts: Initiation of the clotting cascade. *Critical Reviews in Biochemistry and Molecular Biology* **50**(4), 326–336 (may 2015). <https://doi.org/10.3109/10409238.2015.1050550>
39. Spieker, C.J., Závodszy, G., Mouriaux, C., van der Kolk, M., Gachet, C., Mangin, P.H., Hoekstra, A.G.: The effects of micro-vessel curvature induced elongational flows on platelet adhesion. *Annals of Biomedical Engineering* (oct 2021). <https://doi.org/10.1007/s10439-021-02870-4>
40. Springer, T.A.: von willebrand factor, jedi knight of the bloodstream. *Blood* **124**(9), 1412–1425 (aug 2014). <https://doi.org/10.1182/blood-2014-05-378638>
41. Tosenberger, A., Ataulakhanov, F., Bessonov, N., Pantelev, M., Tokarev, A., Volpert, V.: Modelling of thrombus growth in flow with a DPD-PDE method. *Journal of Theoretical Biology* **337**, 30–41 (nov 2013). <https://doi.org/10.1016/j.jtbi.2013.07.023>
42. Tosenberger, A., Ataulakhanov, F., Bessonov, N., Pantelev, M., Tokarev, A., Volpert, V.: Modelling of platelet–fibrin clot formation in flow with a DPD–PDE method. *Journal of Mathematical Biology* **72**(3), 649–681 (may 2015). <https://doi.org/10.1007/s00285-015-0891-2>

43. Ulrichs, H., Udvardy, M., Lenting, P.J., Pareyn, I., Vandeputte, N., Vanhoorelbeke, K., Deckmyn, H.: Shielding of the $\alpha 1$ domain by the α IIb $\beta 3$ domains of von willebrand factor modulates its interaction with platelet glycoprotein α IIb $\beta 3$. *Journal of Biological Chemistry* **281**(8), 4699–4707 (feb 2006). <https://doi.org/10.1074/jbc.m513314200>
44. Xu, S., Xu, Z., Kim, O.V., Litvinov, R.I., Weisel, J.W., Alber, M.: Model predictions of deformation, embolization and permeability of partially obstructive blood clots under variable shear flow. *Journal of The Royal Society Interface* **14**(136), 20170441 (nov 2017). <https://doi.org/10.1098/rsif.2017.0441>
45. Xu, Z., Chen, N., Kamocka, M.M., Rosen, E.D., Alber, M.: A multiscale model of thrombus development. *Journal of The Royal Society Interface* **5**(24), 705–722 (oct 2007). <https://doi.org/10.1098/rsif.2007.1202>
46. Yakusheva, A.A., Butov, K.R., Bykov, G.A., Závodszy, G., Eckly, A., Ataulakhanov, F.I., Gachet, C., Panteleev, M.A., Mangin, P.H.: Traumatic vessel injuries initiating hemostasis generate high shear conditions. *Blood Advances* **6**(16), 4834–4846 (aug 2022). <https://doi.org/10.1182/bloodadvances.2022007550>
47. Yazdani, A., Li, H., Humphrey, J.D., Karniadakis, G.E.: A general shear-dependent model for thrombus formation. *PLOS Computational Biology* **13**(1), e1005291 (jan 2017). <https://doi.org/10.1371/journal.pcbi.1005291>
48. Závodszy, G., van Rooij, B., Azizi, V., Hoekstra, A.: Cellular level in-silico modeling of blood rheology with an improved material model for red blood cells. *Frontiers in Physiology* **8**(AUG) (8 2017). <https://doi.org/10.3389/fphys.2017.00563>
49. Závodszy, G., Van Rooij, B., Czaja, B., Azizi, V., De Kanter, D., Hoekstra, A.G.: Red blood cell and platelet diffusivity and margination in the presence of cross-stream gradients in blood flows. *Physics of Fluids* **31**(3) (3 2019). <https://doi.org/10.1063/1.5085881>